Iodine-123-IPT SPECT Imaging of CNS Dopamine Transporters: Nonlinear Effects of Normal Aging on Striatal Uptake Values

P. David Mozley, Hee-Joung Kim, Ruben C. Gur, Klaus Tatsch, Larry R. Muenz, William T. McElgin, Mei-Ping Kung, Mu Mu, Andrew M. Myers and Hank F. Kung

Departments of Radiology and Psychiatry, University of Pennsylvania, Philadelphia, Pennsylvania; Department of Nuclear Medicine, Asan University, South Korea; Department of Nuclear Medicine, University of Munich, Munich, Germany

Iodine-123-labeled IPT (N-(3-iodopropen-2-yl)-2β-carbomethoxy-3β-(4-chlorophenyl)tropane) is an analog of cocaine that selectively binds the presynaptic dopamine transporter. This study sought to characterize changes in the striatal uptake of IPT with normal aging. **Methods:** The sample included 18 healthy human volunteers. Their ages ranged from 19 to 67 yr. Dynamic SPECT scans of the brain were acquired with about 185 MBq (5 mCi) of IPT on a triple-headed camera. The images were reconstructed with a three-dimensional restorative filter and corrected for attenuation. The mean concentration of radioactivity [μCi/ml] was measured in the head of the caudate and body of the putamen. The remainder of the supratentorial brain was used as a reference. **Results:** The specific uptake of IPT was higher in the caudate than in the putamen of each subject. It decreased significantly with age in both regions. The mean specific uptake in seven volunteers who were less than 30 yr old was 17.6 ± 4.9 in the caudate and 13.3 ± 4.0 in the putamen, compared to only 11.97 ± 3.30 and 7.8 ± 2.68, respectively, in the six middle-aged subjects (t = 2.53 and 2.90, df = 11, p = 0.027 and 0.014). However, there were no significant differences between the six middle-aged subjects and the five volunteers who were older than 60 yr, whose respective means were 9.0 ± 1.6 and 6.2 ± 0.7 (t = 1.83 and 1.28, df = 9, p = 0.10 and 0.23). The results were supported by regression analysis, which indicated that changes with age were not optimally described as a linear function when compared to several nonlinear alternatives. The fit improved when the models accounted for relatively rapid rates of decline during young adulthood, followed by less rapid decline throughout middle age. **Conclusion:** The results are consistent with the findings from previous studies that have shown that the specific uptake values for radiopharmaceuticals that bind the dopamine transporter decline with advancing age. However, results of this study suggest that the effects of aging may be nonlinear and regionally distinct.

Key Words: aging; dopamine transporter; iodine-123-IPT; SPECT

J Nucl Med 1996; 37:1965–1970

The dopamine transporter is a macromolecular complex embedded in the axonal membrane of dopaminergic neurons (*1*). It physically removes free dopamine from the intrasynaptic cleft. When dopamine binds its reuptake sites, an energy-driven process transports the dopamine molecules back into the cytoplasm of the presynaptic buton, where they can be repackaged for retransmission or metabolized (*2,3*). Studies in animals have indicated that transporter-related activity may be the primary mechanism for regulating the tone of the dopaminergic system (*4,5*). In diseases characterized by pathologically low dopaminergic activity (*6–9*), falls in transporter levels have been documented that apparently precede the upregulation of postsynaptic receptor populations (*4*).

Received Aug. 18, 1995; revision accepted May 20, 1996.

For correspondence or reprints contact: P. David Mozley, MD, Division of Nuclear Medicine, 110 Donner Building, H.U.P., 3400 Spruce St., Philadelphia, PA 19104.

Neuroimaging studies have shown that transporter concentrations decline with normal aging in healthy human volunteers (*10–12*). Strong aging effects have been detected with linear models (*10–14*). However, it is possible that nonlinear alternatives would fit some of the data even better, as they do for several dopaminergicly mediated behaviors (*15–19*). Some aging effects could also be regionally distinct, just as some pathological processes appear to effect subregions of the basal ganglia differently (*9,20–23*).

The purpose of this study was to begin characterizing the regional effects of aging on the transporter with ([^{123}I])-labeled IPT (N-(3-iodopropene-2-yl)-2β-carbomethoxy-3β-(4-chlorophenyl)tropane) (Fig. 1). IPT is a tropane analog of cocaine with a binding affinity (K_d) for the transporter of 0.2 n*M* (*24*). Its striatal to cerebellar uptake ratios have averaged 13.1 to 1 at 1 hr postadministration in anesthetized rats (*25*). Preclinical studies in nonhuman primates with SPECT have produced basal ganglia to occipital lobe contrast ratios which averaged 22.8 to 1 at 3 hr postadministration (*26*). Competition studies in animals have shown that the striatal uptake values can be reduced by the administration of indirect dopamine agonists and transporter antagonists (*23,24*). Preliminary studies in healthy volunteers (*27*) and patients with neurodegenerative disorders (Tatsch et al., *personal communication*, 1996) have confirmed that IPT crosses the blood-brain barrier easily in humans. The specific uptake values in the basal ganglia have been high but variable among subjects. This study attempted to estimate how much of the observed variability may be a function of age.

MATERIALS AND METHODS

Subjects

The protocol was approved by the local Human Subjects Committee (IRB) and the Radioactive Drug Research Committee. Informed consent was obtained and documented in writing.

The sample consisted of 18 healthy volunteers. Their ages ranged from 19 to 67 yr; seven were less than 30 yr old; six were between 35 and 48 (mean = 41.5); and five were older than 60 yr (mean = 63.8 yr). There were six women and 12 men, all of whom were subjectively healthy. Their mean educational level was 14.8 ± 2.3 yr (range: 12 to 20 yr). All of them were working, although a 60-yr-old man had retired from the practice of plastic surgery and was only pursuing his second career part time. None of the participants were taking any medications except for three women who used oral contraceptives and one man who took aspirin daily. This 65-yr-old engineer had a history of balloon angioplasty. Otherwise, patients were excluded if they had a history of a disease process that could have affected brain structure or function, including hypertension and diabetes. A standardized review of systems could not elicit a history of nondebilitating ailments such as arthritis, asthma, atopia, chronic constipation or

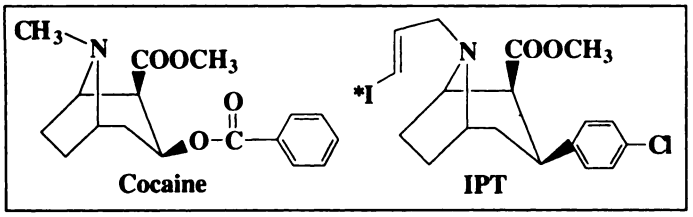

FIGURE 1. Chemical structures of cocaine and [^{123}I]IPT

pain. None of the subjects had a history of a neurological disorder, including head trauma and migraines. None of the subjects had a lifetime history of a psychiatric disorder, including drug abuse, although one man underwent a brief course of couples therapy after his wife had a stillbirth. There were no meaningful abnormalities on their physical examinations. The laboratory studies included urine drug assays, complete blood cell counts, serum electrolyte levels, liver, renal and thyroid function tests, autoimmune screening panels and assays of cortisol, prolactin and reproductive hormones. All values were within normal limits. Only four of the subjects in the youngest age group had not participated in other neuroimaging protocols, which included MRI of the brain. No focal or diffuse abnormalities were found. The older subjects had also participated in studies of regional cerebral blood flow with either PET, SPECT or both, which were normal with no outlying values in any region. All the subjects in the oldest group and three of the middle-aged subjects had also taken extensive neuropsychological tests and no deficits were found.

Radiopharmaceutical

Iodine-123-sodium iodide was obtained commercially. It was produced from an enriched xenon target. The radionuclidic purity was guaranteed to exceed 99.8% at the time of delivery. Theoretically, the specific activity of the ^{123}I was 8.7×10^{18} MBq/mole (2.4×10^{8} mCi/mmole). The IPT precursor was radiolabeled with a process that has already been described (*22,23*). The final product was analyzed for purity by co-injecting a small portion into an HPLC column along with a standard solution of nonradioactive IPT. The final solution was filtered and diluted with normal saline until the concentration reached about 100 MBq per ml. Pyrogenicity tests were performed before administration.

Image Acquisition

Solutions containing the equivalent of 130 mg of potassium iodide were administered orally before the procedure began. A catheter connected to a three-way stopcock was placed in an antebrachial vein and kept patent with warmed normal saline. The subjects were positioned on the imaging table with the assistance of a three-way laser system. Up to 185 MBq (5 mCi) of ^{123}I-labeled IPT were injected as a rapid bolus. The line was flushed with about 20 ml of warmed saline to minimize the transit time from the arm to the heart and decrease the absorption of the radiopharmaceutical by the intravenous tubing and the brachial veins. Scans were performed for 5 min per frame on a triple-headed gamma camera (Prism 3000, Picker Intl., Cleveland, OH) equipped with fanbeam collimators. The acquisition parameters included a 14.5-cm rotational radius, a 20% energy window centered on 159 keV, 120 projection angles over 360° and a 128 × 128 matrix with a pixel width of 2.11 mm in the projection domain. The duration of the procedure was 2 hr in seven subjects; it lasted between 2 and 4 hr in five subjects and for more than 4 hr in three subjects. Three subjects only had 30 min of SPECT data acquired (Fig. 2).

Image Processing and Analysis

The projection images were reconstructed with a standardized protocol that used a counting rate-dependent restoration filter (*28*). The modulation transfer function (MTF) was computed from the line-spread function for the camera and the collimators that were actually used in the study (*29*). Chang's first order method of attenuation was then applied (*30*).

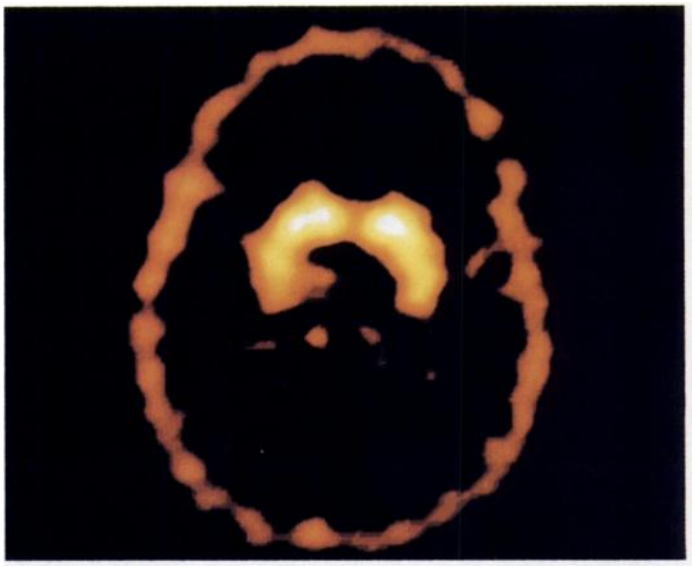

FIGURE 2. IPT SPECT scan of the brain at the level of the basal ganglia in a healthy young adult.

The images were resliced in planes that were parallel to the one containing a line connecting the frontal and occipital poles on the midsagittal section of the first 5-min scan. This orientation was chosen because it tended to be reproducible and produce planes that were roughly parallel to the one containing the line connecting the anterior and posterior commisures (AC-PC line).

The image threshold was set to the most intense pixel in the image, which was always in the caudate. The scans were then magnified in size and displayed on a dichotomous scale that only gave color to a pixel if it contained 50% or more of the mean counts in the brightest pixel. A software package that has already been described was used to place ROIs on the images (*31*). Cross-registration with identically formatted MRI scans in nine subjects showed that the high-contrast ratios on the IPT images led to significant blooming artifacts. This problem with volume averaging made it appear as if the basal ganglia could be visualized about 4–6 mm above and below their true anatomical boundaries. For this reason, all ROIs were smaller than the actual size of the structures they represented. The region for the caudate was limited exclusively to the four to six central slices through its anterior-most head. When the mean counts in a slice dropped to below 33% of the mean value in the two central slices, it was excluded from the analysis. Blooming also obscured the boundary between the putamen and the globus pallidus. Because its medial border could not be identified, the ROI for the putamen was limited to the lateral aspect of the lenticular nucleus posterior to the caudate. Because there was spillover of counts across the genu of the internal capsule, the distance between the ROIs for the caudate and putamen was widened artificially to about 5 mm. The ROI for the putamen that was used in the analysis represented the central portion within the plane and did not include the most posterior portion of ganglia where the activity usually appeared differentially low (Fig. 3).

There were not enough counts in the calcarine cortex to use it as a reference region. Only 1 to 4 counts per pixel per 5-min image could be detected in the reconstruction domain, so that fluctuations of only 1 count sometimes changed the calculated concentration of radioactivity in this region by a factor of 2. The larger ROI for the cerebellum produced somewhat more stable time-activity curves, even though the mean concentration of radioactivity in it was

FIGURE 3. Image of a 48-yr-old, right-handed woman shows the contrast between different subregions of the basal ganglia.

essentially identical to the mean concentration in the calcarine strip. However, volume averaging from nonspecific activity in the bone marrow of the skull became a problem at some of the later time points, making it appear as if the concentration of radioactivity in the posterolateral cerebellar rim was increasing. For these reasons, nonspecific activity was estimated by drawing a large ROI around the whole supratentorial brain (WB) which excluded the basal ganglia and thalamus. This region always had a slightly higher concentration of radioactivity in it when compared to the calcarine cortex or cerebellum, but it consistently produced more stable time-activity curves (Fig. 4).

Mean counting rates in the reconstruction domain were converted into units of concentration from calibration factors for the camera and the well counter. The calibration factors were generated from images of uniform phantoms containing known amounts of ^{123}I that were acquired, processed and analyzed with parameters identical to those used to study the human volunteers.

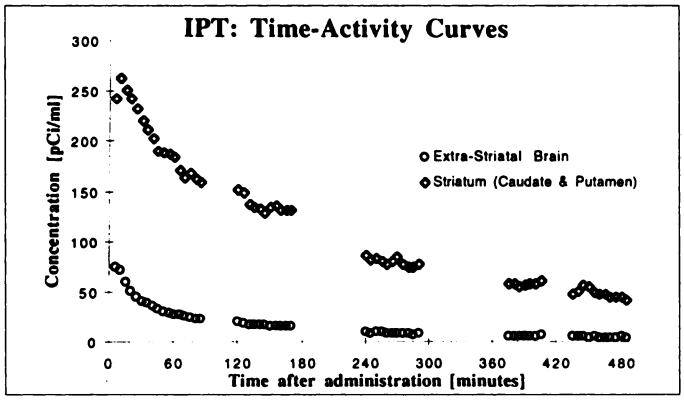

FIGURE 4. Time-activity curves in a healthy 24-yr-old man. Sixty-two SPECT scans were intermittently acquired for 5 min each during the first 8 hr after the intravenous administration of 176 MBq (4.77 mCi) [^{123}I]IPT.

Statistical Analyses

Specific uptake was defined by subtracting the mean concentration of radioactivity in the background from the mean concentration in each basal ganglia region and then dividing the result by the mean concentration in the background region ((mean ROI-mean Bkgd) ÷ mean Bkgd). Values were calculated independently for the caudate and putamen at each time point. The data that were acquired between 90 and 120 min after injection were averaged to produce the final outcome measure. The two subjects who participated in prolonged image acquisition protocols were given short rest breaks during part of this interval. In these cases, the outcome measure was generated by extrapolating the curves from the time of peak basal ganglia activity across the break into the curves for the remainder of the study.

Specific uptake values in the middle-aged subjects were compared to the means in the younger and older groups using two-tailed, independent t-tests. This was complemented by curve fitting to define mathematical functions that described the relationships between regional basal ganglia uptake and age. Five models were used:

1. $y = a + b*age$.
2. $y = a + b*age + c*age^2$.
3. $y = a*exp(b*age)$.
4. $y = a_0 + b_0*age$ for age $< x$ and $y = a_1 + b_1*age$ for age $> x$.
5. $y = a_0 + b_0*age + c_0*age^2$ for age $< x$ and $y = a_1 + b_1*age$ for age $> x$,

where Model 1 describes a straight line with a slope of b and a y-intercept at the end of adolescence of a, Model 2 is a quadratic that reduces to a linear equation when $c = 0$, Model 3 is a monoexponential function, Model 4 is a broken stick consisting of two straight lines with an elbow at some age x and Model 5 is a variant with a quadratic equation fit to the data up until some age x and a linear model applied after the age x with a slope of b_1. Models 2–5 were considered as alternatives to the linear relationship represented by the first equation.

RESULTS

Image analysis showed that IPT uptake in the brain was rapid. The fraction of the injected dose in the brain reached a maximum of 15% at 15–20 min after injection. The time to peak basal ganglia activity varied from 10 min in a subject less than 30 yr old to 50 min in a subject more than 60 yr old. In every subject, the activity in the caudate was more intense than in any other region of the brain. The highest caudate-to-background contrast ratio measured was 33:1 at 3 hr postadministration. The specific uptake between 90 min and 2 hr postadministration was less and varied from 6.7 to 24.6 with a mean value of 13.0 ± 4.0. The most variability was found in the group of young adults less than 30 yr old, where the specific activity in the caudate ranged from 12.7 to 24.6.

Uptake in the putamen was always less intense than the activity in the head of the caudate. The distribution of activity in the putamen rarely appeared uniform. Left-right asymmetries in the posterior aspect of the putamen were frequently pronounced. The images in Figure 3 are typical because they appear to show a gradient of activity with significantly less radioactivity in the posterior portion of the putamen than in the anterior portion. The specific uptake in the relatively small ROI representing the central portion of the putamen varied from 5.3 to 21.4 with a mean of 9.21 ± 3.4.

The relationships between age and the specific activity in the caudate and putamen are shown in Figure 5. Virtually none of the subjects over 35 yr of age had specific-activity values that

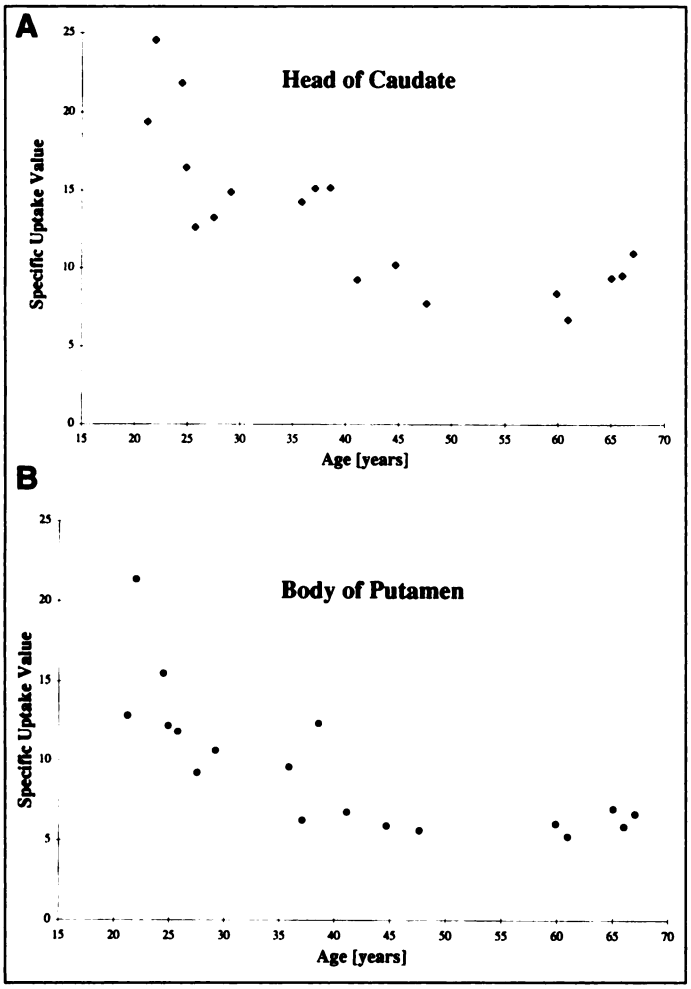

FIGURE 5. (A) Relationship between age and specific uptake in the head of the caudate. (B) Specific uptake in the putamen is less than that in the caudate. There is essentially no difference between the values in early and late middle age.

were as high as the values in the youngest adults. The mean specific activity in the seven volunteers, who were less than 30 yr old, was 17.59 ± 4.9 in the caudate and 13.3 ± 4.03 in the putamen, compared with only 11.97 ± 3.30 and 7.77 ± 2.68, respectively, in the six middle-aged subjects ($t = 2.53$ and 2.90, $df = 11$, $p = 0.027$ and 0.014). However, there were no significant differences between the six middle-aged subjects and the five volunteers older than 60 yr, whose means were 9.00 ± 1.58 and 6.18 ± 0.68 ($t = 1.83$ and 1.28, $df = 9$, $p = 0.10$ and 0.23), respectively. A linear relationship between IPT contrast and aging could be described as a straight line with a slope of -0.22 per year in the caudate and -0.18 per year in the putamen. The R^2 values for a straight line were 0.60 for the caudate and 0.55 for the putamen. However, each of the nonlinear models fit the data better, as shown in Tables 1 and 2. In each table, the five models can be compared by scanning from left to right in the same row.

The results show that the linear model does not fit the data as well as several alternatives. The quadratic model adds another term, which has a p value of 0.012 for the caudate and 0.008 for the putamen. The exponential model also fits better than the linear one, but, with the same number of coefficients, the R^2 values only increase by 4% and 9% for the caudate and putamen, respectively. The sample size was too small to determine the precise age at which the decline with age tends to level. However, if 35 yr of age had been used as a break point, then the slope of the line for the caudate would have been -1.2 per year in young adults, compared to only -0.15 in volunteers between 35 and 67 yr old. In the putamen, the slope in adults less than 35 yr would have been -0.96, compared to only -0.08 in older volunteers. Using the quadratic-then-linear model, the R^2 values ranged from 0.68 to 0.71 for the caudate ($p < 0.001$) and 0.67 to 0.69 for the putamen ($p < 0.001$), depending on the age chosen as the cutoff point.

TABLE 1
Models Describing Relationships with Normal Aging in the Caudate

	Linear	Quadratic	Exponential	Stick	Quadratic line
Standard deviation	3.22	2.67	3.05	2.64	2.74
R^2	0.60	0.74	0.66	0.75	0.71
Adjusted r^2	0.58	0.71	0.62	0.72	0.70
F-statistic	24.2	21.7	28.1	22.4	20.33
Degrees of freedom	1, 16	2, 15	1, 16	2, 15	2, 15

DISCUSSION

Studies with several different dopamine transporter ligands have consistently shown that striatal uptake values decrease with age (*10–14*). However, the linear model did not fit the IPT data as well as any of the nonlinear alternatives. Most of the aging effects were found during young adulthood. The rate of decline throughout middle age was significantly slower.

Similar effects of aging on other components of the dopaminergic system have been reported. Normal aging curves produced with [^{11}C]raclopride, a D2 dopamine receptor antagonist, show the same phenomenon (*32,33*). Behavioral studies have found that several dopaminergically mediated motor skills do not decline linearly with advancing age (*15–19*). Studies of dopaminergic axon function have shown a substantial amount of overlap between the striatal uptake values of [^{11}C]fluorodopa in older and middle-aged volunteers (*34–36*). In one longitudinally followed sample, the specific uptake values actually seemed to increase slightly with age in four of 10 healthy volunteers (*37*). A relatively marked decline during young adulthood followed by significantly slower decreases throughout middle age could partially explain these observations and help explain why some investigators have not found evidence of a decline with advancing age at all (*38*).

Several other factors may also partially explain why nonlinear relationships with age have not been emphasized by many earlier studies. The stability of IPT uptake values during middle age was observed in a group of healthy workers. A healthy worker effect has been documented in many research settings (*39–41*). It can influence outcome because the fraction of the population that works is generally more vigorous than the whole population from which the workers are drawn. This study excluded people who were not employed, as well as workers with relatively minor health problems. This feature of the

TABLE 2
Models Describing Relationships with Normal Aging in the Putamen

	Linear	Quadratic	Exponential	Stick	Quadratic line
Standard deviation	2.98	2.42	2.85	2.55	2.40
R^2	0.55	0.72	0.61	0.69	0.69
Adjusted r^2	0.52	0.68	0.61	0.65	0.68
F-statistic	19.3	19.2	27.3	16.6	19.6
Degrees of freedom	1, 16	2, 15	1, 16	2, 15	2, 15

design precluded the detection of another drop late in life, because the oldest subject was only 67. It may also have had an impact on several biological variables that contribute to the measurements indirectly, or in other words independently of the concentration of transporters.

The striatal uptake values of IPT are clearly related to the concentration of available dopamine transporter binding sites (*42–44*). However, specific uptake values are also dependent on blood flow. Regional cerebral perfusion determines the fraction of the dose delivered to the target tissues and influences the rate at which unbound radioactivity is eliminated. If age-related decrements in cerebral perfusion had decreased the delivery of the tracer to the basal ganglia or reduced the rate of clearance from the background ROI, then the uptake values in older subjects would have been artifactually lower. The rate of decline with aging would have been exaggerated and appeared more, not less, linear. This may not have been a significant problem in this study because none of the older subjects had any perfusion abnormalities on earlier studies of blood flow.

Cerebrospinal fluid (CSF) expansion could have reduced the apparent concentration of unbound radioactivity in the whole-brain background regions more than in the centers of the basal ganglia. The effect would have been to artifactually inflate the specific uptake values in direct proportion to the amount of cerebral atrophy. Ventricular dilatation would have had the opposite effect. The striatal uptake values would have been artifactually reduced because imperfect resolution causes some volume averaging with the adjacent CSF in the lateral ventricular horns. Ventricular dilatation would have had a greater effect on the values for the caudate than for the putamen. However, the observation that the IPT uptake values in the caudate were higher than those in the putamen of every subject suggests that this was not a problem. The effect of ventricular dilatation would have been compensated for by the punch biopsy approach to region sampling, which kept the ROIs in the center of each basal ganglia. However, no signs of CSF expansion were noted on the MRI scans of any of the subjects in the oldest age group. These observations suggest that, while several technical and biological factors unrelated to transporter binding may have influenced the specific uptake values, the magnitude of their effects may not be enough to completely account for the nonlinearity of the findings.

These extraneous contributions to the uptake values could affect each transporter ligand differently. IPT has already been shown to have several unique pharmacokinetic properties which make its whole-body distribution, retention and elimination distinctive when compared to several other radiopharmaceuticals for imaging the transporter (*27*). This makes it possible that the findings of nonlinearity apply specifically to measurements with IPT and not to the true concentration of dopamine transporters. However, the similarity between the results of this study and the effects of aging on dopaminergic behavior suggest that nonlinear models should be tested in future studies of the transporter.

CONCLUSION

The results are consistent with the findings from several previous studies that have shown that the specific uptake values for radiopharmaceuticals that bind the CNS dopamine transporter decline with advancing age. However, results of this study with IPT suggest that the effects of aging may be nonlinear and regionally distinct.

ACKNOWLEDGMENTS

This study was partially supported by National Institutes of Health grant NS-24538 and National Institute of Mental Health grant MH-43880. The clinical laboratory studies performed by the General Clinical Research Center at the University of Pennsylvania Medical Center were made possible by National Institutes of Health grant MO1-RR00040. We are grateful to Picker International for maintaining the instrumentation and contributing to the development of the image processing algorithms.

REFERENCES

1. Giros B, Caron MG. Molecular characterization of the dopamine transporter. *Trends Pharmac Sci* 1993;14:43–49.
2. Feldman RS, Quenzer LF. Catecholamines. In: *The fundamentals of neuropsychopharmacology*. Sunderland, MA: Sinauer Associates, Inc.; 1984: 183–187.
3. Johanson CE, Fischman M. The pharmacology of cocaine related to its abuse. *Pharmacol Rev* 1989;41:3–52.
4. Donnan GA, Woodhouse DG, Kaczmarczyk SJ, et al. Evidence for plasticity of the dopaminergic system in Parkinsonism. *Mol Neurobiol* 1991;5:421–433.
5. Giros B, Jaber M, Jones SR, Wightman RM, Caron MG. Hyperlocomotion and indifference to cocaine and methamphetamine in mice lacking the dopamine transporter. *Nature* 1996;379:606–612.
6. Hantraye P, Brownell AL, Elmaleh D, et al. Dopamine fiber detection by [^{11}C]-CFT and PET in a primate model of Parkinsonism. *Neuroreport* 1992;3(3):265–268.
7. Frost JJ, Rosier AJ, Reich SG, et al. PET imaging of the dopamine transporter with ^{11}C-WIN 35,428 reveals marked decline in mild Parkinson's disease. *Ann Neurol* 1993;34:423–431.
8. Shoemaker H, Pimoule C, Arbilla S, Scatton B, Javoy-Agid F, Langer SZ. Sodium dependent [^{3}H] cocaine binding associated with dopamine uptake sites in the rat striatum and human putamen decrease after dopaminergic denervation and in Parkinson's disease. *Naunyn-Schmiedeberg's Arch Pharmacol* 1985;239:227–235.
9. Innis RB, Seibyl JP, Scanley BE, et al. SPECT imaging demonstrates loss of striatal dopamine transporters in Parkinson disease. *Proc Natl Acad Sci USA* 1993;90:11965–11969.
10. van Dyck CH, Seibyl JP, Malison RT, et al. Age-related decline in striatal dopamine transporter binding with I-123-b-CIT SPECT. *J Nucl Med* 1995;36:1175–1181.
11. Volkow ND, Fowler JS, Wang GJ, et al. Decreased dopamine transporters with age in healthy human subjects. *Ann Neurol* 1994;36:237–239.
12. Volkow ND, Ding Y-S, Fowler JS, et al. Dopamine transporters decrease with age. *J Nucl Med* 1996;37:554–559.
13. Kaufman MJ, Madras BK. [^{3}H]CFT ([^{3}H]WIN 35,428) accumulation in dopamine regions of monkey brain: comparison of a mature and an aged monkey. *Brain Res* 1993;611:322–325.
14. Shimuzu I, Prasad C. Relationship between [^{3}H]mazindol binding to dopamine uptake sites and [^{3}H]dopamine uptake in rat striatum during aging. *J Neurochem* 1991;56:575–579.
15. Lezak MD. *Neuropsychological assessment*, 2nd ed. New York, NY: Oxford University Press; 1983.
16. Bak JS, Greene RL. Changes in neuropsychological functioning in an aging population. *J Consult Clin Psych* 1980;48:395–399.
17. Harley JP, Leuthold CA, Matthews CG, Bergs LE. *Wisconsin neuropsychological test battery T-score norms for older Veterans Administration Medical Center patients*. Madison, WI: CG Matthews; 1980.
18. Heaton RK, Grant I, Matthews CG. Differences in neuropsychological test performance associated with age, education and sex. In: Grant I, Adams KM, eds. *Neuropsychological assessment of neuropsychiatric disorders*. New York, NY: Oxford University Press; 1986; 100–120.
19. Heaton RK, Grant I, Matthews CG. *Comprehensive norms for an expanded Halstead-Reitan Battery*. Odessa, FL: Psychological Assessment Resources, Inc.; 1991; 5–13.
20. Goeders NE, Kuhar MJ. Chronic cocaine administration induced opposite changes in dopamine receptors in the striatum and nucleus accumbens. *Science* 1983;221:773–775.
21. Leenders KL, Salmon EP, Tyrrell P, et al. The nigrostriatal dopaminergic system assessed in vivo by PET in healthy volunteer subjects and patients with Parkinson's disease. *Arch Neurol* 1990;47:1290–1298.
22. Patel J, Trout SJ, Kruk ZL. Regional differences in evoked dopamine efflux in brain slices of rat anterior and posterior caudate putamen. *Arch Pharmacol* 1992;346:267–276.
23. Kordower JH, Freeman TB, Snow BJ, et al. Neuropathological evidence of graft survival and striatal reinnervation after the transplantation of fetal mesencephalic tissue in a patient with Parkinson's disease. *N Engl J Med* 1995;332:1118–1124.
24. Kung M-P, Essman WD, Frederick D, et al. IPT: a novel iodinated ligand for the CNS dopamine transporter. *Synapse* 1995;20:316–324.
25. Goodman MM, Kung M-P, Kabalka GW, Kung HF, Switzer R. Synthesis and characterization of radioiodinated N-(3-Iodopropen-1-yl)2B-carbomethoxy-3B-(4-chlorophenyl) tropanes: potential dopamine reuptake site imaging agents. *J Med Chem* 1994;37:1535–1542.
26. Malison RT, Vessotskie JM, Kung M-P, et al. Striatal dopamine transporter imaging in nonhuman primates with [I-123] IPT SPECT. *J Nucl Med* 1995;36:2290–2297.
27. Mozley PD, Stubbs JB, Kim H-J, et al. Biodistribution and dosimetry of [I-123]-labeled IPT. *J Nucl Med* 1996;37:151–160.
28. Kim H-J, Karp JS, Mozley PD, et al. Simulating Tc-99m cerebral perfusion studies with a three-dimensional Hoffman brain phantom: collimator and filter selection in SPECT neuroimaging. *Ann Nucl Med* 1996;10:153–160.
29. Kim HJ, Karp JS, Kung HF, Mozley PD. Quantitative effects of a count rate dependent

Wiener filter on image quality: a basal ganglia phantom study simulating [I-123] dynamic SPECT imaging [Abstract]. *J Nucl Med* 1993;34(suppl):190.
30. Chang LT. A method for attenuation correction in radionuclide computed tomography. *IEEE Trans Nucl Sci* 1978;NS-25:638–643.
31. Resnick SR, Karp JS, Turetsky BI, Gur RE. Comparison of anatomically defined versus physiologically based regional localization: effects on PET-FDG quantitation. *J Nucl Med* 1993;34:2201–2207.
32. Antonini A, Leenders KL. Dopamine D2 receptors in normal human brain: effect of age measured by PET and [^{11}C]-raclopride. *Ann New York Acad Sci* 1993;695:81–85.
33. Antonini A, Leenders KL, Reist H, Thomann R, Beer HF, Locher J. Effect of age on D2 dopamine receptors in normal human brain measured by PET and ^{11}C-raclopride. *Neurology* 1993;50:474–480.
34. Martin WRW, Palmer MR, Patlak CS, Calne DB. Nigrostriatal function in man studied with PET. *Ann Neurol* 1989;26:535–542.
35. Sawle GV, Colebatch JG, Shah A, et al. Striatal function normal aging: Implications for Parkinson's disease. *Ann Neurol* 1990;28:799–804.
36. Cordes M, Snow BJ, Cooper S, et al. Age-dependent decline of nigrostriatal dopaminergic function: a PET study of grandparents and their grandchildren. *Ann Neurol* 1994;36:667–670.
37. Vingerhoets FJG, Snow BJ, Lee CS, Schulzer M, Mak E, Calne DB. Longitudinal fluorodopa PET studies of the evolution of idiopathic Parkinsonism. *Ann Neurol* 1994;36:759–764.
38. Eidelberg D, Takikawa S, Dhawan V, et al. Striatal fluorine-18-DOPA uptake: absence of an aging effect. *J Cereb Blood Flow Metab* 1993;13:881–888.
39. Choi BC. Definition, sources, magnitude, effect modifiers and strategies of reduction of the healthy worker effect. *J Occup Med* 1993;35:890–892.
40. Blanc PD, Katz P, Yelin E. Mortality risk among elderly workers. *Am J Industrial Med* 1994;26:543–547.
41. Arrighi MH, Hertz-Picciotto I. The evolving concept of the healthy worker survivor effect. *Epidemiology* 1994;5:189–196.
42. Kim H-J, Mozley PD, McElgin W, et al. In vivo quantification of presynaptic dopamine transporter binding parameters in human brains with [I-123]IPT SPECT [Abstract]. *J Nucl Med* 1995;36(suppl):125P.
43. Kim H-J, Mozley PD, Kung M-P, et al. Absolute activity measurements of in vivo monkey brain using a triple-headed SPECT and a new radioligand: [I-123]IPT [Abstract]. *J Nucl Med* 1995;36(suppl):178–179.
44. Kushner SA, Frederick D, Kung M-P, et al. Quantitative [I-123]IPT SPECT measurements: comparisons with ex vivo dissection and in vitro binding assays in nonhuman primates [Abstract]. *J Nucl Med* 1996;37(suppl):66P.

Prediction of Radiation Doses from Therapy Using Tracer Studies with Iodine-131-Labeled Antibodies

Diane A. DeNardo, Gerald L. DeNardo, Aina Yuan, Sui Shen, Sally J. DeNardo, Daniel J. Macey, Kathleen R. Lamborn, Marc Mahe, Mark W. Groch and William D. Erwin

Department of Internal Medicine, University of California Davis Medical Center, Sacramento, California; Department of Radiation Physics, MD Anderson Cancer Center, Houston, Texas; Brain Tumor Research Center, University of California San Francisco, San Francisco, California; Rush-Presbyterian St. Lukes Medical Center, Rush University, Chicago, Illinois; Siemens Medical Systems, Nuclear Medicine Engineering, Hoffman Estates, Illinois

Tracer pharmacokinetic studies are often used in treatment planning for radionuclide therapy including radioimmunotherapy. This study evaluates the validity of using tracer studies to predict radiation doses from therapy with the same radiolabeled antibody. **Methods:** Quantitative imaging and blood radioactivity were used to obtain the pharmacokinetics and radiation doses that were delivered to the total body, blood, marrow, lungs, liver, kidneys, thyroid, spleen and tumors. Tracer and therapy data for eight patients with lymphoma and one patient with breast cancer were compared using linear regression statistics. Doses of ^{131}I-labeled antibody for the tracer studies ranged from 0.1 to 0.4 GBq (2 to 10 mCi), and therapy doses ranged from 0.7 to 5.6 GBq (20 to 150 mCi). **Results:** Radiation doses to tissues and, in particular, the bone marrow and tumors were reliably predicted from tracer studies. In this group of patients, median dose to marrow from marrow targeting, total body and blood was 9.2 cGy/GBq for tracer studies and 7.6 cGy/GBq for therapy studies with a median difference of 0.5 cGy/GBq. Median dose to tumors was 81.1 cGy/GBq for tracer studies and 70.3 cGy/GBq for therapy studies with a median difference of 5.9 cGy/GBq. **Conclusion:** In these patients, tracer studies were predictive of the radiation doses from therapy for total body, major organs and tumors. The radiation doses to marrow and tumors, which are the usual determinants of the therapeutic index, correlated well between tracer and therapy studies ($r \geq 0.95$).

Key Words: iodine-131; radioimmunotherapy; antibody; radiation dosimetry; treatment planning; therapeutic nuclear medicine

J Nucl Med 1996; 37:1970–1975

Radionuclide therapies, such as radioimmunotherapy, require treatment planning that would be improved if radiation doses from the therapeutic dose could be predicted from a tracer dose. Radiation doses depend on pharmacokinetics that may be unique for each patient as well as for each radiopharmaceutical. For example, radiation dose to normal marrow cells incident to targeting of ^{131}I-labeled antibody on malignant cells in the marrow is unique for each patient (*1*).

Protocols that administer marrow-ablative radiation doses have utilized imaging data from tracer studies to determine the antibody and radionuclide dose to be given for subsequent therapy, using a predetermined ceiling on the estimated radiation doses delivered to the critical organs. Eary et al. (*2*) have administered therapy doses of ^{131}I-labeled antibody as large as 22.2 GBq (600 mCi) that delivered up to 1500 cGy to normal organs. Tracer studies were used to select for treatment those patients that showed favorable tumor-to-nontumor localization of the radiolabeled antibody and to determine the amount of antibody and of ^{131}I to be administered.

Tracer studies would be very useful to predict radiation doses from therapy if the pharmacokinetics are the same for tracer and therapy amounts of the radiopharmaceutical (*3*); equivalence has not been documented adequately yet for radiolabeled antibodies. The purpose of this study was to assess the predictive value of the tracer data for the dosimetry of the therapy dose.

MATERIALS AND METHODS

Patients

Patients were selected for this study from a larger group of patients treated with ^{131}I-labeled Lym-1 or ChL6 antibodies because: (a) imaging and blood data commencing immediately after injection were available for 7 days for both the tracer and the therapy studies; (b) the same amount of antibody preload was used

Received Nov. 14, 1995; revision accepted Apr. 4, 1996.
For correspondence or reprints contact: Gerald L. DeNardo, MD, 1508 Alhambra Blvd., Rm. 214, Sacramento, CA 95816.